Stevanović, N. R.; Apostolović, D.; Milčić, M. K.; Lolić, A.; Hage, M. van; Ćirković-Veličković, T.; Baošić, R. Interaction, Binding Capacity and Anticancer Properties of N,N′-Bis(Acetylacetone)-Propylenediimine-Copper(II) on Colorectal Cancer Cell Line Caco-2. *New Journal of Chemistry* **2021**, *45* (14), 6231–6237. https://doi.org/10.1039/D1NJ00040C.

Interaction, binding capacity and anticancer properties of *N,N′*-bis(acetylacetone)-propylenediimine-copper(II) on colorectal cancer cell line Caco-2

Nikola Stevanović[a], Danijela Apostolović[b], Miloš Milčić[c], Aleksandar Lolić[c], Marianne van Hage[b], Tanja Ćirković Veličković[c,d,e,f], and Rada Baošić[c*]
[a] Analysis, Gandijeva 76a, Belgrade, Serbia
[b] Immunology and Allergy Divison, Department of Medicine Solna, Karolinska Institutet, Stockholm, Sweden
[c] University of Belgrade – Faculty of Chemistry, Studentski trg 12-16, Belgrade, Serbia
[d] Serbian Academy of Science and Art, Belgrade, Serbia
[e] Faculty of Bioscience Engineering, Ghent University, Ghent, Belgium
[f] Ghent University Global Campus, Incheon, South Korea
* author for correspondence: rbaosic@chem.bg.ac.rs

Abstract

Different Schiff base complexes have biological activity which makes them suitable for drug design. The biological properties of tetradentate Schiff base copper(II) complexe with *N,N′*-bis(acetylacetone)propylenediimine, has been studied. The cytotoxic activity on Caco-2 cells determined by MTT, Anexin V and PI apoptosis assays. The *N,N′*-bis(acetylacetone)propylenediimine-copper(II) showed the anti-cancer and anti-proliferative properties by inducing apoptosis in Caco-2 cells. A comparison of the cytotoxic activity of this compound with cisplatin shows that is more effective on colorectal cancer cell line Caco-2. The binding capacity and interaction of *N,N′*-bis(acetylacetone)propylenediimine-copper(II) with HSA were systemically investigated by *in vitro* fluorescence spectroscopy, and CD spectroscopy, and *in silico* molecular docking study. Furthermore, *in vitro* and *in silico* interaction studies indicated that complex is binding to the HSA with the static quenching mechanism without changes of protein conformation. Calculated number of binding sites was in line with molecular docking studies. Obtained Ka value suggests that compound can be released from protein in target cells. It shown that tetradentate Schiff base copper(II) complex possess *in vitro* biological activities against cancer epithelial cells which depends on molecular structure of complex,

causing apoptosis, and they are able to bind to the protein drug carrier in circulation to the target tissue.

Keywords

Schiff base complexes, Copper(II) complex, Cytotoxic activity, Human serum albumin, Molecular docking

Highlights

- *N,N′*-bis(acetylacetone)propylenediimine-copper(II) bind to HSA
- Schiff base Cu(II) complex possess *in vitro* biological activities against cancer cells
- Minimum changes in % of *α*-helixes during formation of protein-compound complex
- *N,N′*-bis(acetylacetone)propylenediimine-copper(II) induces apoptosis

Graphical abstract

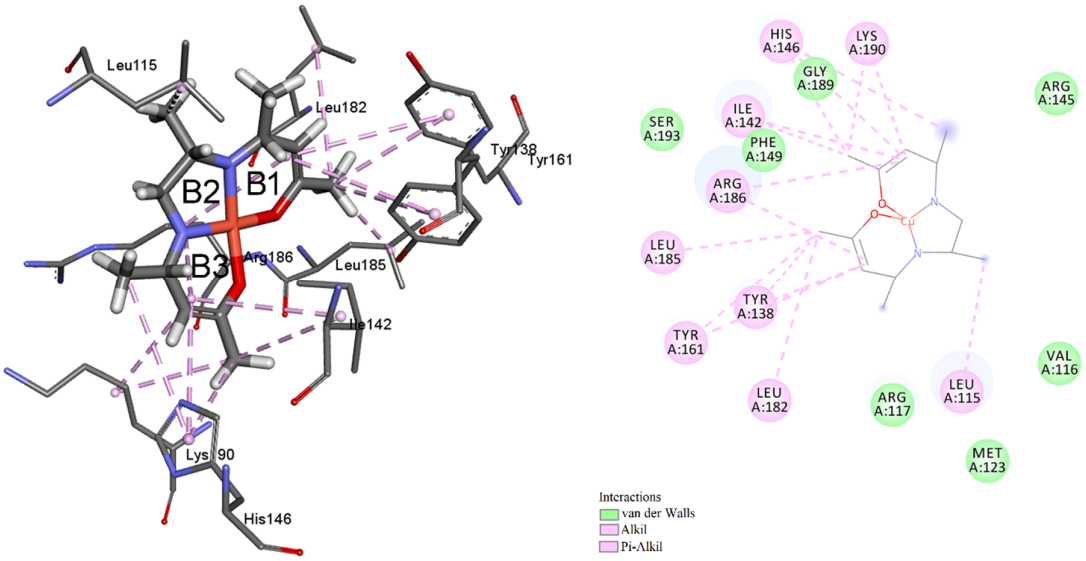

The biological properties of *N,N′*-bis(acetylacetone)propylenediimine-copper(II) complex, their anti-proliferative and anticancer potential as well as the effect of structure on this potential were main goal. The binding capacity and interaction of *N,N′*-bis(acetylacetone)propylenediimine-copper(II) with HSA were systemically investigated *in vitro* and *in silico*.

1. Introduction

Schiff bases and their complexes with different metal ions show a wide range of biological activities, including antitumor, anti-bacterial, antiviral, fungicidal and anticarcinogenic properties, and therefore play an important role in the field of drug design [1–4]. Although Schiff base can build complex compounds with many transition metals, preference of ions like Cu(II), Co(II), Ni(II) and Mn(II) over the other, is ultimately due to their flexibility to more than one coordination geometries and the ability to exist in multiple oxidation states [5,6]. The organic ligands such as Schiff bases, introduced into complex could regulate metal uptake, transfer, function, and excretion in biological systems, which may limit the side effects and provide better activities in drug resistance cells [7]. The diversity of Schiff bases and their metal complexes provides wide prospects for the design of novel compounds with unique structures, different functional characteristics in order to improve biological activities [8].

The copper is endogenous, bioessential element and therefore less toxic than platinum. It has considerable redox potentials with selective permeability to membranes of cancer cells [9,10]. Schiff base Cu(II) complexes combined with different moieties revealed great potential for antiproliferative, antibacterial, and gastroprotective activity [11,12] and have been studied on various cancer cell lines with relatively low IC_{50} values [7,13–15]. Therefore, investigation of the Schiff base copper complexes has the potential for discovering new chemicals with strong anticancer activities as potential alternative strategy to platinum agents.

Human serum albumin (HSA) is a single polypeptide globular protein constituent of blood plasma. It was reported that majority of drugs travel in plasma and reach the target tissues by binding to HSA. This means that the drug distribution is somewhat controlled by HSA [16]. The 3D structure of HSA showed that protein has three homologous domains (I-III) where each of it can be divided into two subdomains, A and B [17,18]. Binding sites for most aromatic and heterocyclic ligands are mainly located within two hydrophobic pockets in subdomains IIA

(Sudlow's site I) and IIIA (Sudlow's site II) [19,20]. Understanding of the noncovalent and reversible interactions of small molecules with proteins such as HSA is essential for studying both biochemical processes and biological activity.

In this study the anti-proliferative and anticancer potential on colorectal cancer cells of tetradentate Schiff base copper(II) complex with *N,N′*-bis(acetylacetone)ethylenediimine as ligand, were investigated. Interaction and binding capacity of this Schiff base copper(II) complex with HSA were systemically investigated by fluorescence spectroscopy, CD spectroscopy, and molecular docking study under simulative physiological condition.

2. Material and methods

2.1. Materials

Fetal calf serum (FCS), penicillin, streptomycin, L-glutamate, nonessential amino acids, 3-(4,5-dimethylthiazol-2-yl)-2,5-diphenyltetrazolium bromide (MTT), Ficoll-Paque density gradient media, trypan blue dye, dimethyl-sulfoxide (DMSO) and Human serum albumin (HSA) were purchased from Sigma Aldrich (St. Louis, MO, USA). AIM V serum free medium and Dulbecco's modified Eagle medium (DMEM) were obtained from Life Technologies, Inc. (Rockville, MD; USA). Annexin V and propidium iodide (PI) were purchased from Becton Dickinson Bioscience (BD, Bioscience, San Jose, CA, USA). Caco-2 (human epithelial colorectal adenocarcinoma cells) was obtained from American Type Culture Collection (Manassas, VA, USA).

2.2. Schiff base copper(II) complex

Schiff base copper(II) complex with *N,N′*-bis(acetylacetone)propylenediimine as ligand were synthesized according to previously reported procedure [21,22] (Figure S1).

2.3. Cell culture

Colorectal cancer cell line Caco-2 cells (ATCC® HTB-37™) were grown in T-75 bottle with modified DMEM medium (10% FCS, 1% streptomycin, 1% penicillin, and 1% nonessential amino acids). They were incubated at 37℃ in a humidified atmosphere with 5% CO_2.

2.4. MTT assay

Caco-2 cells were seeded (200.000 cells per well) in 96-well plates for 24 h at 37℃ in a humidified atmosphere with 5% CO_2. Cells were stimulated with different concentrations of copper(II) complex in 1% DMSO in DMEM medium (0.01-1000 μg/mL), previously filtered through 0.2 μm filter. Untreated control samples were cells with 1% DMSO, positive control were cells pretreated with 50% of DMSO. A solution of MTT (3-(4,5-dimethyl-2-thiazolyl)-2,5-diphenyltetrazoliumbromide) (5mg/mLin PBS) was added to each well and mixed with well content to allow the metabolization of MTT. After the incubation, the medium was removed, and formazan was resuspended in 100 μL DMSO. The absorbance, which represents the number of viable cells, was read at 550 nm and the background subtracted at 620 nm. The cytotoxicity was represented as IC_{50} value (concentration which inhibits cell growth by 50%). All experiments were performed in triplicate (SDs between measurements are less than 15%).

2.5. Annexin V assay

The induced apoptosis ability of complex on Caco-2 was determined by a flow cytometry with Annexin V-FITC and propidium iodide (PI), according to manufacturer's instructions (BD Bisciene, San Jose, CA, USA). Briefly, 200 000 cells, treated with various concentrations of complex (0.01 and 0.1 μg/mL) for 24 and 48 h, were harvested and washed out with PBS. Thereafter, cells were resuspended in binding buffer containing Annexin V and PI, incubated for 20 minutes, and analyzed by flow cytometry using FACSCanto II cytometer (BD Bioscience). The FlowJo v10 software (TreeStar *Inc.,* Ashland*,* USA) was used to analyze the data. Controls

were unstained cells, cells stained with Annexin V and cells stained with PI. The experiment was performed in duplicate.

2.6. Fluorescence spectroscopy and quenching analysis

Concentration of HSA in PBS was determined by UV absorbance at 280 nm (ε = 35,700 M^{-1} cm^{-1}). Fluorescent spectra of HSA (1 μM) and investigated complexes (concentration range 0.5-35 μM) were recorded on FluoroMax-4 spectrofluorometer (Horiba Scientific, Kyoto, Japan). All experiments were carried out at room temperature in a 3.5 mL quartz cuvette using 5 nm slit. Fluorescence spectra were recorded under the following conditions: excitation wavelength 280 nm and emission wavelength 290-500 nm. A blank was made for each concentration of compound, in which protein solution was replaced with PBS. Blank spectrum was subtracted from the emission spectra of the corresponding protein:compound solution. All experiments were performed in duplicate and data analyzed and graphed by OriginPro8 software (Northampton, MA, USA). Quenching data were analyzed according to Stern-Volmer method using the following equation $F_0 / F = 1 + K_{sv} [Q]$, where F_0 and F are the fluorescence intensities before and after addition of a quencher, *Ksv* is the Stern-Volmer quenching constant and *[Q]* is the concentration of the quencher [23,24]. Further calculations were done according to literature [25].

2.7. Circular dichroism measurements

The circular dichroism (CD) spectra were recorded on the JASCO J-715 spectropolarimeter (JASCO, Tokyo, Japan), previously calibrated with a 0.6 g/L solution of ammonium D-10-camphorsulfonate. The samples were analyzed in a 0.1 mm path length quartz cell at 25°C. Far-UV spectra were collected in 0.1 nm steps at a rate of 50 nm/min over the wavelength range 195–260 nm. CD spectra were obtained for mixture of HSA:compound in molar ratios: 1:0; 1:0.1; 1:0.5; 1:1 and 1:5 in PBS. HSA concentration was 10 μM. Each spectrum was acquired four

times, and results were averaged and expressed as residue-average molar ellipticity [26,27]. Calculation of percentage of secondary structures was performed with CONTIN algorithm, the reference protein set SP29 (29 soluble proteins) was selected [28].

2.8. Computational analysis

Geometries of the investigated copper complexes were optimized in our previous study with DFT method [29]. The 3D crystal structure of HSA was obtained from Protein Data Bank (PDB), PDB code 1BM0 [30,31]. The protonation state of each titratable amino acid was estimated by finite difference Poisson-Boltzmann (FDPB) continuum electrostatics method inplemented in H++ program (version 3.2) [32]. Amino acids from N- and C-terminus missing from the crystal structure were built in and the protein structure was optimized in CHARMM program (version c35b1) using the CHARM22 protein force feld [33]. Optimization was carried out in 3000 optimization steps (1000 steps with steepest-descent algorithm followed by 2000 steps with Newton–Raphson algorithm). The optimized structures of metal complexes and protein were prepered for docking in AutoDockTools program. The „partial charges“ were assigned to atoms by fitting the atomic charges to quantum-mechanically calculated molecular electrostatic potential using RESP scheme [34]. The blind docking study was done on the grid centered on the protein center (dimension 80 x 80 x 80 Å) using AutoDock4 program [30].

3. Results and discussion

3.1. Interaction, binding capacity and conformation of HSA with presence of [Cu(acac$_2$pn)]

Interaction of [Cu(*acac*$_2$pn)] with human serum albumin as one of drug carrier protein was followed *in vitro* with fluorescence spectroscopy. Increasing the concentration of [Cu(*acac*$_2$pn)] in solution, quenching the tryptophan emission spectra was observed. The maximum of emission λ_{max} showed red shift from 337 nm to 342 nm (Fig. 1A).

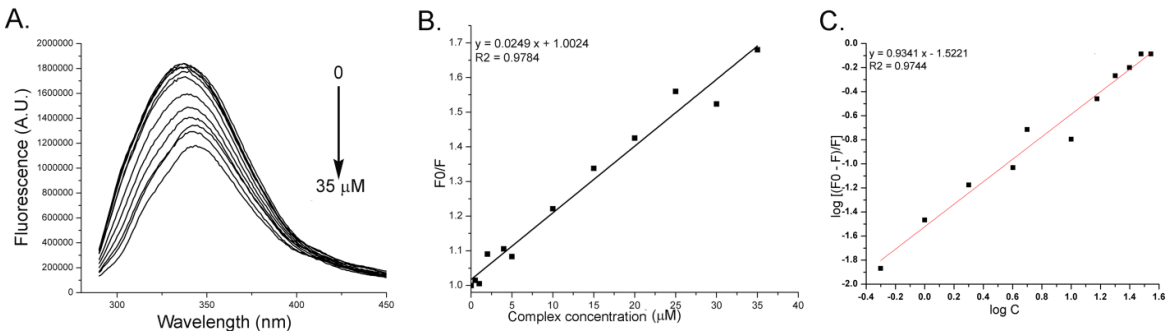

Figure 1. Fluorescence quenching study of [Cu(*acac*$_2$pn)] on HSA. A) Emission spectra of 1µM HSA with [Cu(*acac*$_2$pn)] in concentration range of 0.5-35µM B) Stern-Volmer plot for determination of *Ksv*; C) double-logarithmic graph for calculations of *Ka* and *n*.

The decrease of λ_{max} for 13.8% was noticed when HSA:[Cu(*acac*$_2$pn)] ratio was 1:10. This result indicates formation of protein-compound complex. Applying Stern-Volmer equation allows us to calculate Stern-Volmer constant (*Ksv*=2.5·10^4 M^{-1}). Furthermore, there was a linear dependence between fluorescence intensities before and after addition of a quencher (*Fo/F*) at the different concentrations of [Cu(*acac*$_2$pn)] (Fig. 1B). A linear Stern-Volmer plot can be obtained in cases of static or collisional quenching [35,36]. Assuming the observed changes in fluorescence come from the interaction between [Cu(*acac*$_2$pn)] and protein, the Stern-Volmer constant (*Ksv*) can be interpreted as the binding constant of the complex formation [23]. Obtained Stern-Volmer plot here were linear and therefore the fluorescence quenching rate constant (*kq*) can be calculated if τ_0 (fluorescence lifetime of fluorophore without a quencher) is known according to equation $K_{sv} = kq \cdot \tau_0$ [36], based on which the constant of quenching rate could be calculated (*kq* = 4.4·10^{12} M^{-1} s^{-1}). If the value of the quenching rate constant (*kq*) is higher than diffusion-limited quenching (for water is a 10^{10} M^{-1} s^{-1}) it implies that there is a complex formation.

Static mechanism of fluorescence quenching happens mostly due to formation of non-fluorescence protein-compound complex [37]. That allowed us to use double-logarithmic equation $log\ [(F_0 - F) / F] = log\ K_a + n \cdot log[Q]$ [35]. The intercept provides the binding constant (*Ka*=3.1·10^4 M^{-1}) and the slope of the double logarithmic plot yields the number of binding sites

(n=0.93) (Fig. 1C). Calculated *Ka* showed lower values in comparison to non-covalent interaction between avidin-biotin (10^{15} M^{-1}) [38], which suggest that compound could release from protein in target cells, as it was showed before. There were several studies where Cu(II) complexes of Schiff bases binds to HSA and quench the Trp_{214} fluorescence, as well that compound could bind to the specific protein domain, leading to the conclusion that protein-compound complex can be transported and dispositioned into the blood circulation [39–41].

HSA has a major role as protein carrier for drugs, peptides, and small molecules allowing them to circulate through circulatory system long enough as its half-life [42]. In order to determine does [Cu($acac_2$pn)] change and makes the protein conformation unstable, a far UV CD spectrum of 1 μM HSA with different molar ratio of [Cu($acac_2$pn)] were recorded (Fig. 2). The CD spectra of HSA alone showed two minima in the UV region at 208 nm and 222 nm, characteristic of the α-helical structure of protein, as shown before [43].

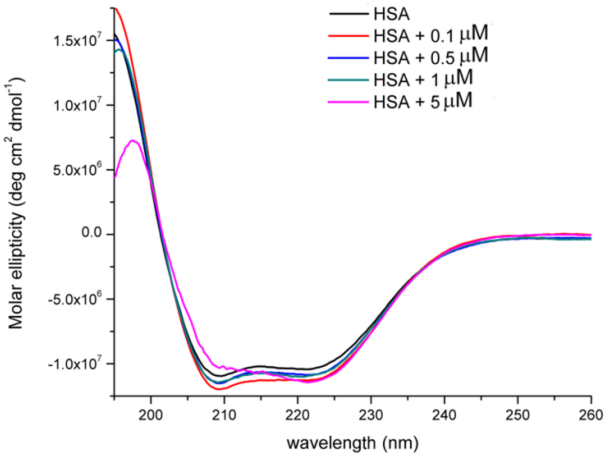

Figure 2. CD spectrum of HSA with different molar ratio of [Cu($acac_2$pn)]

By adding the [Cu($acac_2$pn)], in different ratio, a slight conformational change was observed. The addition of [Cu($acac_2$pn)] to HSA leads to a minimum decrease in negative and positive ellipticity of minima without any significant protein spectrum shape change. The content of the secondary structures (Table 1), showed that a slight changes in protein conformation happens, and that was most obvious in protein:compound complex with molar ratio 1:5. When this ratio is

1:1, percentage of α-helixes decrease from 52.1% to 50.7%, and percentage of β-turn increased from 18.5% to 20.1%. Still, the predominance structure is of α-helix and this minimum changes in of percentage of α-helixes during the formation of protein-compound complex represent the ability of protein to bind a compound and stabilize the protein structure. Similar minimal changes in HSA conformation during complex formation were reported earlier [44].

Our results directly imply that binding of [Cu(*acac*$_2$pn)] to HSA will not only influence the protein's ability to bind this compound but influence stability and longevity of the protein in plasma.

Table 1. Secondary structures of HSA after addition of [Cu(*acac*$_2$pn)]

Molar ratio	% of secondary structure			
HSA to [Cu(*acac*$_2$pn)]	α-helix	β-sheet	β-turn	Random coil
1:0	52.1	8.7	18.5	22.7
1:0.1	54.4	6.5	17.0	22.1
1:0.5	50.6	7.2	18.7	22.5
1:1	50.7	7.3	20.1	21.9
1:5	40.2	4.1	20.9	34.8

3.2. Molecular docking of the [Cu(acac$_2$pn)] with HSA

Molecular docking has been employed in order to understanding interaction between [Cu(*acac*$_2$pn)] and HSA which is responsible for the transportation of drugs. Detailed of molecular docking showed that the test compound [Cu(*acac*$_2$pn)] binds to HSA on subdomain IB (Fig. 3).

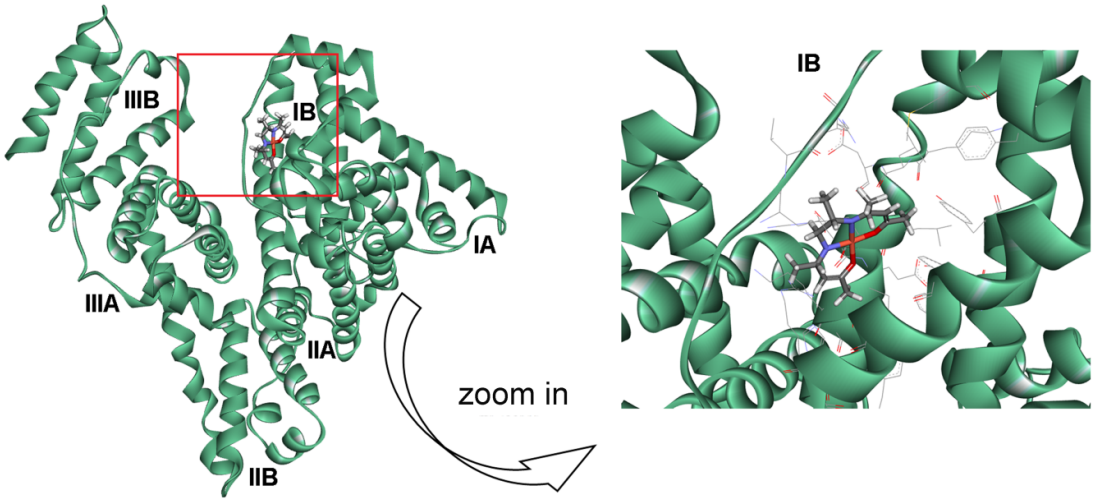

Figure 3. Complex HSA-[Cu(*acac*$_2$pn)] and binding site

Sudlow site I, so-called warfarin-binding site is well known as binding site for heterocyclic anionic ligands and some drugs, while subdomain IB is binding site for heme [19]. The binding site, alkyl interactions and 2D diagram of the most important interaction are shown on Fig. 4. A high-affinity binding site is located between the following amino acids: charged, polar, and amino acids with the pyrrole group Lys$_{90}$, Tyr$_{138}$, His$_{146}$, Tyr$_{161}$, Arg$_{186}$; nonpolar Leu$_{115}$, Ile$_{142}$, Leu$_{182}$, Leu$_{185}$. It was observed that the complex was positioned closest to the position located between Leu$_{182}$ and Arg$_{186}$ and that most protein-compound interactions take place between the chelate rings of the [Cu(*acac*$_2$pn)] (B1 and B3) while the propylenediamine bridge ring (B2) only interacts with Leu$_{115}$ (Fig. 4A). π interactions of B1 chelate ring with with residues of amino acid Leu$_{182}$, Leu$_{185,}$ as well as with phenyl groups of Tyr$_{138}$ and Tyr$_{161}$ are achieved. The chelating ring B3 interacts with the residue Lys$_{90}$, the pyridine residue His$_{146}$, as well as with Ile$_{142}$. From the 2D diagram (Fig. 4B) it is concluded that Leu$_{115}$, His$_{146}$ Ile$_{142}$ and Arg$_{186}$ are amino acids that stabilize the resulting complex between the [Cu(*acac*$_2$pn)] and HSA. In addition to alkyl and π-alkyl interactions, van der Walls interactions with the following amino acids were observed: Val$_{116}$, Arg$_{117}$, Met$_{123}$, Arg$_{145}$, Phe$_{149}$, Gly$_{189}$ and Ser$_{193}$.

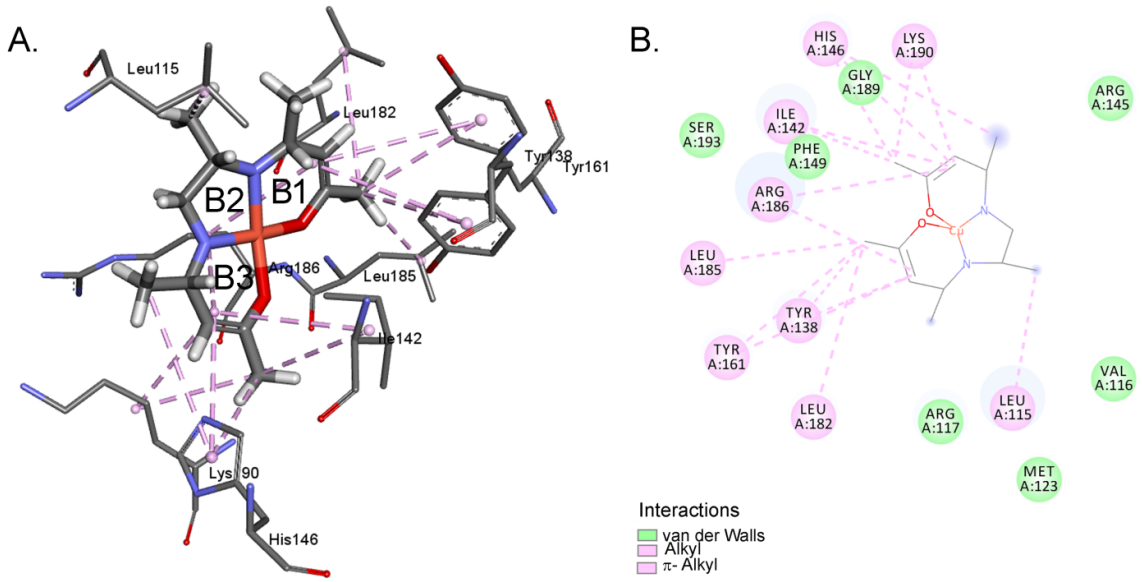

Figure 4. Interactions of HSA from subdomain IB with [Cu(*acac*$_2$pn)]

A) binding site and alkyl interactions B) 2D diagram with most important interactions.

In several studies, ligand binding to HSA has been shown to stabilize its conformation, such as vitamin B12 [45], fatty acids [46], lupeol [47] and phloretin [48]. The results obtained are in accordance with the data reported in the literature, which defines a similar behaviour of the Cu (II) complex with 1,1-*0*-phenanthroline, as well as the Cu(II)-epigallocatehingalate complex [49,50].

3.3. Tetradentate Schiff base copper(II) complex show cytotoxic and anti-proliferative activity on colorectal cancer epithelial cells Caco-2

In order to evaluate the anti-proliferative and anticancer potential of the investigated tetradentate Schiff base [Cu(*acac*$_2$pn)] complex, the synthesized compound was tested for cytotoxicity against Caco-2 cells. The cytotoxic activities were determined by MTT assay and values were expressed as IC_{50} values from the dose response curve (Figure S2). Tested compound elicited a significant cytotoxicity and cell inhibitory effect after 24h and 48h of treatment on Caco-2 cell. The IC_{50} values was 0.02 µg/mL (0.05µM) and 0.61 µg/mL (1.80µM), for 24h and 48h incubation time, respectively. The results indicated that the Schiff base complex induced an

antiproliferative effect on human colon cancer cells in a time and dose-dependent manner. More importantly, [Cu(*acac*$_2$pn)] showed almost 100-fold higher cytotoxicity in comparison to the observed values with cisplatin on Caco-2 cells (for 24h IC_{50} 120.9 μM and for 48h 93.5 μM) [51]. Obtained IC_{50} values are in line with study performed with $Cu(BrHAP)_2$ complex on HT-29 cell line, another colorectal cancer cell line [52]. Furthermore, complex showed to have greater cytotoxicity than [Cu(L)(phen)] complex on mouse fibroblast's cells L929 and human breast cancer cell line MCF-7 even after 48h [53].

According to concept of cell permeability the most important parameters that govern transmembrane diffusion are polarity and size. The cell lipid membrane favors the passage of lipophilic materials thus lipo-solubility is an important factor which controls the bioactivity together with size and steric effects of molecule [54,55]. In the [Cu(*acac*$_2$pn)], presence of enantiomeric center in diamine bridge, probably causes further deviation from square-planar geometry due to steric clashing with methyl group from chelate ring influencing strongly on cell viability on Caco-2 cells.

In order to investigate what type of cytotoxic effects of [Cu(*acac*$_2$pn)] complex have on the cells we preformed an Anexin V and PI assay on Caco-2 cells at concentrations closest to IC_{50} value (0.1 and 0.01 μg/ml, respectively, Fig. 5).

When we investigated the induction of apoptosis, after 24h of incubation with [Cu(*acac*$_2$pn)], no necrotic cells were observed in comparison with the control (1% DMSO, Fig.S4). In the control (unstimulated cells Fig 5) there was about 27% of pre-apoptotic cells detected, which could be due to overlap FITC and PI channel (Fig. S3). This did not affect the results since in general in unstimulated group there was very small amount of apoptotic cells (ap to 5% in 48h incubation), there were no necrotic cells, and overall sum of pre- and apoptotic cells is much higher in treated cells than in control (Fig. 5). The presentage of the pre-apoptotic cells was much higher when the cells were treted with lower dose for 24h (0.01 μg/ml, Fig. 5A), and in general looking into the % of pre- and apopotic cells toghether, this conetration induced slightly higher programmed cell

death. After 48h of the incubation with [Cu(*acac*$_2$pn)] there was a small percentage of the necrotic cells, but also percentage of the live cells increased in comparison to the amount of the cells which entered into the apoptosis (Fig. 5B). This was in line with MTT assay where the IC_{50} value increased, probably due to some proliferative effect, explaining short effectivnes of the complex.

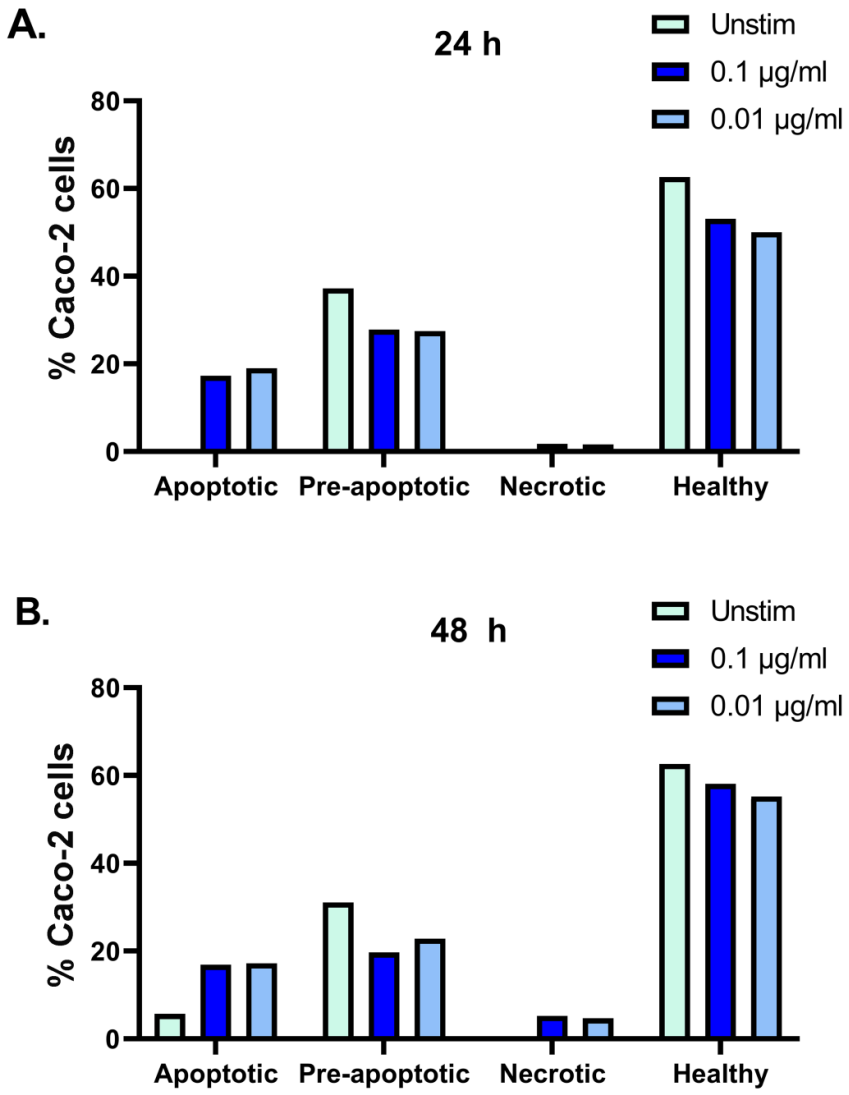

Figure 5. Apoptotic effect of [Cu(*acac*$_2$pn)] on Caco-2 cell line after: 24h (panel A) and 48h of incubation (panel B)

Induction of programmed cell death specific to cancer cells could be due to presence of enantiomeric center on carbon atom of methyl group in diamine bridge and the deviation from square-planar geometry [56]. Propylenediamine in the bridge due to asymmetry in structure, gives possibility of conformational rotation of [Cu(*acac*$_2$pn)] during interaction with cell membrane.

4. Conclusion

Here we showed that thetradentate Schiff base copper(II) complex [Cu(*acac*$_2$pn)] interact with HSA as a protein carrier and binds with non-covalent interactions. Data from fluorescence spectroscopy and quenching study showed a static quenching mechanism, where calculated *Ka* value suggests that compound could be released from protein in target cells. Molecular docking showed that the test compound [Cu(*acac*$_2$pn)] binds to HSA on subdomain IB, where the CD spectroscopy confirmed no changes in the protein structure. Furhteremore, [Cu(*acac*$_2$pn)] possess significant cytotoxic activity to colorectal cancer cell line Caco-2, in comparison to cisplatin, and can induce apoptosis to some extent. The results from the current study suggest that [Cu(*acac*$_2$pn)] can be effective and promising as novel anticancer drugs and further investigation should occur.

Conflict of interest

The authors declare no conflict of interest.

Acknowledgment

This study was supported by the following funds: the Swedish Research Council, the Swedish Heart-Lung Foundation, the Konsul Th C Bergh Foundation, Tore Nilsson Foundation, the Swedish Cancer and Allergy Foundation, the European Union's Horizon 2020 FoodEnTwin project, GA No. 810752, Karolinska Institutet Research Foundation Grant, and Ministry of

Education, Science and Technological Development of Republic of Serbia, Contract number: 451-03-9/2021-14/200168. The EC does not share responsibility for the content of the article.

References

1 M. M. Abd-Elzaher, A. A. Labib, H. A. Mousa, S. A. Moustafa, M. M. Ali and A. A. El-Rashedy, *Beni-Suef Univ. J. Basic Appl. Sci.*, 2016, **5**, 85–96.

2 O. Andersen, *Chem. Rev.*, 1999, **99**, 2683–2710.

3 A. Jarrahpour, D. Khalili, E. De Clercq, C. Salmi and J. Brunel, *Molecules*, 2007, **12**, 1720–1730.

4 C. Marchand, J. A. Beutler, A. Wamiru, S. Budihas, U. Mollmann, L. Heinisch, J. W. Mellors, S. F. Le Grice and Y. Pommier, *Antimicrob. Agents Chemother.*, 2008, **52**, 361–364.

5 M. A. Malik, O. A. Dar, P. Gull, M. Y. Wani and A. A. Hashmi, *Medchemcomm*, 2018, **9**, 409–436.

6 S. Abyar, A. A. Khandar, R. Salehi, S. Abolfazl Hosseini-Yazdi, E. Alizadeh, M. Mahkam, A. Jamalpoor, J. M. White, M. Shojaei, O. Aizpurua-Olaizola, R. Masereeuw and M. J. Janssen, *Sci. Rep.*, 2019, **9**, 1–11.

7 W. J. Lian, X. T. Wang, C. Z. Xie, H. Tian, X. Q. Song, H. T. Pan, X. Qiao and J. Y. Xu, *Dalt. Trans.*, 2016, **45**, 9073–9087.

8 S. Konstantinovic, B. Radovanovic, Z. Cakic and V. Vasic, *J. Serbian Chem. Soc.*, 2003, **68**, 641–647.

9 S. Kacar, H. Unver and V. Sahinturk, *Arab. J. Chem.*, 2020, **13**, 4310–4323.

10 A. F. Shoair, A. A. El-Bindary, N. A. El-Ghamaz and G. N. Rezk, *J. Mol. Liq.*, 2018, **269**, 619–638.

11 A. M. Abu-Dief and I. M. A. Mohamed, *Beni-Suef Univ. J. Basic Appl. Sci.*, 2015, **4**, 119–133.

12 O. Krasnovskaya, A. Naumov, D. Guk, P. Gorelkin, A. Erofeev, E. Beloglazkina and A. Majouga, *Int. J. Mol. Sci.*, 2020, **21**, 3965-4002.

13 C. Fan, H. Su, J. Zhao, B. Zhao, S. Zhang and J. Miao, *Eur. J. Med. Chem.*, 2010, **45**, 1438–1446.

14 C. Santini, M. Pellei, V. Gandin, M. Porchia, F. Tisato and C. Marzano, *Chem. Rev.*, 2014, **114**, 815–862.

15 A. Hussain, M. F. AlAjmi, M. T. Rehman, S. Amir, F. M. Husain, A. Alsalme, M. A. Siddiqui, A. A. AlKhedhairy and R. A. Khan, *Sci. Rep.*, 2019, **9**, 1–17.

16 W. Zhang, F. Wang, X. Xiong, Y. Ge and Y. Liu, *J. Chil. Chem. Soc.*, 2013, **58**, 1717–1721.

17 A. Bujacz, *Acta Crystallogr. Sect. D Biol. Crystallogr.*, 2012, **68**, 1278–1289.

18 X. M. He and D. C. Carter, *Nature*, 1992, **358**, 209–215.

19 G. Sudlow, D. J. Birkett and D. N. Wade, *Mol. Pharmacol.*, 1975, **11**, 824–32.

20 F. Zsila, *Mol. Pharm.*, 2013, **10**, 1668–1682.

21 R. Baošić, D. Milojković-Opsenica and Ž. Tešić, *J. Planar Chromatogr. – Mod. TLC*, 2003, **16**, 412–416.

22 A. E. M. P.J. McCarthy, R.J. Hovey, K. Ueno, *J. Am. Chem. Soc.*, 1955, **77**, 5820–5824.

23 I. Hasni, P. Bourassa, S. Hamdani, G. Samson, R. Carpentier and H.-A. Tajmir-Riahi, 2011, **126,** 630-639**.**

24 L. Liang, H. A. Tajmir-Riahi and M. Subirade, *Biomacromolecules*, 2008, **9**, 50–56.

25 J. Vesic, I. Stambolic, D. Apostolovic, M. Milcic, D. Stanic-Vucinic and T. Cirkovic Velickovic, *Food Chem.*, 2015, **185**, 309–317.

26 D. Stanic-Vucinic, I. Prodic, D. Apostolovic, M. Nikolic and T. Cirkovic Velickovic, *Food Chem.*, 2013, **138**, 590–599.

27 D. Stanic-Vucinic, M. Stojadinovic, M. Atanaskovic-Markovic, J. Ognjenovic, H. Grönlund, M. van Hage, R. Lantto, A. I. Sancho and T. C. Velickovic, *Mol. Nutr. Food*

Res., 2012, **56**, 1894–1905.

28 M. Stojadinovic, L. Burazer, D. Ercili-Cura, A. Sancho, J. Buchert, T. C. Velickovic and D. Stanic-Vucinic, *J. Sci. Food Agric.*, 2012, **92**, 1432–1440.

29 N. M. Aburas, N. R. Stevanović, M. K. Milčić, A. D. Lolić, M. M. Natić, Ž. L. Tešić and R. M. Baošić, *J. Braz. Chem. Soc.*, 2013, **24,** 1322-1333.

30 G. M. Morris, R. Huey, W. Lindstrom, M. F. Sanner, R. K. Belew, D. S. Goodsell and A. J. Olson, *J. Comput. Chem.*, 2009, **30**, 2785–2791.

31 S. Sugio, A. Kashima, S. Mochizuki, M. Noda and K. Kobayashi, *Protein Eng.*, 1999, **12**, 439–46.

32 R. Anandakrishnan, B. Aguilar and A. V. Onufriev, *Nucleic Acids Res.*, 2012, **40**, W537–W541.

33 B. R. Brooks, R. E. Bruccoleri, B. D. Olafson, D. J. States, S. Swaminathan and M. Karplus, *J. Comput. Chem.*, 1983, **4**, 187–217.

34 C. I. Bayly, P. Cieplak, W. Cornell and P. A. Kollman, *J. Phys. Chem.*, 1993, **97**, 10269–10280.

35 J. R. Lakowicz, *Principles of fluorescence spectroscopy*, Kluwer Academic/Plenum, 1999.

36 J. R. Lakowicz, I. Gryczynski, Z. Gryczynski and J. D. Dattelbaum, *Anal. Biochem.*, 1999, **267**, 397–405.

37 A. B. T. Ghisaidoobe and S. J. Chung, *Int. J. Mol. Sci.*, 2014, **15**, 22518–38.

38 O. Livnah, E. A. Bayer, M. Wilchek and J. L. Sussman, *Proc. Natl. Acad. Sci. U. S. A.*, 1993, **90**, 5076–80.

39 P. K. B. Sartaj Tabassum,Musheer Ahmad, Mohd Afzal, Mehvash Zaki, *J. Photochem. Photobiol. B Biol.*, 2014, **140**, 321–331.

40 V. C. da Silveira, G. F. Caramori, M. P. Abbott, M. B. Gonçalves, H. M. Petrilli and A. M. da Costa Ferreira, *J. Inorg. Biochem.*, 2009, **103**, 1331–1341.

41 M. Li, S. Huang, C. Ye and Y. Xie, *Spectrochim. Acta Part A Mol. Biomol. Spectrosc.*,

2015, **150**, 290–300.

42 S. L. Minic, M. Milcic, D. Stanic-Vucinic, M. Radibratovic, T. G. Sotiroudis, M. R. Nikolic and T. Ć. Velickovic, *RSC Adv.*, 2015, **5**, 61787–61798.

43 M. Radibratovic, S. Minic, D. Stanic-Vucinic, M. Nikolic, M. Milcic and T. Cirkovic Velickovic, *PLoS One*, 2016, **11**, e0167973.

44 J. Sochacka and W. Baran, *Protein J.*, 2012, **31**, 689–702.

45 H.-N. Hou, Z.-D. Qi, Y.-W. OuYang, F.-L. Liao, Y. Zhang and Y. Liu, *J. Pharm. Biomed. Anal.*, 2008, **47**, 134–139.

46 T. R. C. Guizado, *J. Mol. Model.*, 2014, **20**, 2450.

47 M. Kallubai, A. Rachamallu, D. P. Yeggoni and R. Subramanyam, *Mol. Biosyst.*, 2015, **11**, 1172–83.

48 D. Barreca, G. Laganà, G. Toscano, P. Calandra, M. A. Kiselev, D. Lombardo, E. Bellocco, A. Angell, S. Magazù and F. Migliardo, *BBA - Gen. Subj.*, 2017, **1861**, 3531–3539.

49 N. Shahabadi, B. Bazvandi and A. (Arman) Taherpour, *J. Coord. Chem.*, 2017, **70**, 3186–3198.

50 A. Singha Roy, K. S. Ghosh and S. Dasgupta, *J. Biomol. Struct. Dyn.*, 2013, **31**, 1191–1206.

51 K. H. Leong, C. Y. Looi, X.-M. Loong, F. K. Cheah, U. Supratman, M. Litaudon, M. R. Mustafa and K. Awang, *PLoS One*, 2016, **11**, e0152652.

52 M. Hajrezaie, M. Paydar, S. Zorofchian Moghadamtousi, P. Hassandarvish, N. S. Gwaram, M. Zahedifard, E. Rouhollahi, H. Karimian, C. Y. Looi, H. M. Ali, N. Abdul Majid and M. A. Abdulla, *Sci. World J.*, 2014, **2014**, 1–12.

53 F. Mohammadizadeh, S. K. Falahati-pour, A. Rezaei, M. Mohamadi, M. R. Hajizadeh, M. R. Mirzaei, A. Khoshdel, M. A. Fahmidehkar and M. Mahmoodi, *BioMetals*, 2018, **31**, 233–242.

54 N. J. Yang and M. J. Hinner, Getting Accros the Cell Membrane: An Overview for Small Molecules, Peptides and Proteins, 2015, pp. 29–53.

55 Z. Uyar, D. Erdener, İ. Koyuncu and Ü. Arslan, *J. Turkish Chem. Soc. Sect. A Chem.*, 2017, 963–980.

56 A. Ehnbom, S. K. Ghosh, K. G. Lewis and J. A. Gladysz, *Chem. Soc. Rev.*, 2016, **45**, 6799–6811.